

Melatonin alleviates vascular calcification and ageing through exosomal miR-204/miR-211 cluster in a paracrine manner

Feng Xu¹ | Jia-Yu Zhong² | Xiao Lin³ | Su-Kang Shan¹ | Bei Guo¹ | Ming-Hui Zheng¹ | Yi Wang¹ | Fuxingzi Li¹ | Rong-Rong Cui¹ | Feng Wu⁴ | En Zhou⁵ | Xiao-Bo Liao⁶ | You-Shuo Liu² | Ling-Qing Yuan¹ 

¹Department of Metabolism and Endocrinology, National Clinical Research Center for Metabolic Diseases, Hunan Provincial Key Laboratory of Metabolic Bone Diseases, The Second Xiang-Ya Hospital, Central South University, Changsha, China

²Department of Geriatrics, Institute of Aging and Age-related Disease Research, The Second Xiang-Ya Hospital, Central South University, Changsha, China

³Department of Radiology, The Second Xiang-Ya Hospital, Central South University, Changsha, China

⁴Department of Pathology, The Second Xiang-Ya Hospital, Central South University, Changsha, China

⁵Department of Otorhinolaryngology Head and Neck Surgery, Hunan Provincial People's Hospital, Changsha, China

⁶Department of Cardiovascular Surgery, The Second Xiang-Ya Hospital, Central South University, Changsha, China

Correspondence

Ling-Qing Yuan, Department of Metabolism and Endocrinology, National Clinical Research Center for Metabolic Diseases, Hunan Provincial Key Laboratory of Metabolic Bone Diseases, The Second Xiangya Hospital, Central South University, Changsha, Hunan Province 410011, China.
Email: allenylq@csu.edu.cn

You-Shuo Liu, Department of Geriatrics, Institute of Aging and Age-related Disease Research, The Second Xiang-Ya Hospital, Central South University, Changsha, Hunan Province 410011, China.
Email: liuyoushuo@csu.edu.cn

Funding information

This work is funded by the National Natural Science Foundation of China (grant numbers 81770881 and 81870623) and the Fundamental Research Funds for the Central Universities of Central South University Grant 2018zzts048).

Abstract

In the elderly with atherosclerosis, hypertension and diabetes, vascular calcification and ageing are ubiquitous. Melatonin (MT) has been demonstrated to impact the cardiovascular system. In this study, we have shown that MT alleviates vascular calcification and ageing, and the underlying mechanism involved. We found that both osteogenic differentiation and senescence of vascular smooth muscle cells (VSMCs) were attenuated by MT in a MT membrane receptor-dependent manner. Moreover, exosomes isolated from VSMCs or calcifying vascular smooth muscle cells (CVSMCs) treated with MT could be uptaken by VSMCs and attenuated the osteogenic differentiation and senescence of VSMCs or CVSMCs, respectively. Moreover, we used conditional medium from MT-treated VSMCs and Transwell assay to confirm exosomes secreted by MT-treated VSMCs attenuated the osteogenic differentiation and senescence of VSMCs through paracrine mechanism. We also found exosomal miR-204/miR-211 mediated the paracrine effect of exosomes secreted by VSMCs. A potential target of these two miRs was revealed to be BMP2. Furthermore, treatment of MT alleviated vascular calcification and ageing in 5/6-nephrectomy plus high-phosphate diet-treated (5/6 NTP) mice, while these effects were partially reversed by GW4869. Exosomes derived from MT-treated VSMCs were internalised into mouse artery detected by in vivo fluorescence image, and these exosomes reduced vascular calcification and ageing of 5/6 NTP mice, but both effects were largely abolished by

Xu and Zhong equally contributed to this work.

This is an open access article under the terms of the Creative Commons Attribution-NonCommercial License, which permits use, distribution and reproduction in any medium, provided the original work is properly cited and is not used for commercial purposes.

© 2020 The Authors. *Journal of Pineal Research* published by John Wiley & Sons Ltd

inhibition of exosomal miR-204 or miR-211. In summary, our present study revealed that exosomes from MT-treated VSMCs could attenuate vascular calcification and ageing in a paracrine manner through an exosomal miR-204/miR-211.

KEYWORDS

ageing, BMP2, exosomes, melatonin, miR-204/miR-211, vascular calcification

1 | INTRODUCTION

In the elderly with atherosclerosis, hypertension, diabetes, macroangiopathy, and chronic kidney disease, vascular calcification and ageing are ubiquitous.¹ The degree of vascular calcification is closely related to cardiovascular mortality and amputation and is an important factor in determining the health of the elderly. Osteogenic differentiation of vascular smooth muscle cells (VSMCs) is the key cytological foundation of vascular calcification.² Vascular ageing is a degenerative change in the structure and function of the cardiovascular system. Moreover, vascular calcification, an important phenotype of vascular ageing,³ is a complex and adjustable biological process that is regulated by various microRNA (miRNA) networks.⁴ However, the role and mechanisms of vascular calcification and ageing remain unknown.

Vascular smooth muscle cells are the main cells of the vascular wall, which play an indispensable role in maintaining the stability of structure and function of blood vessels.⁵ Vascular calcification and other dysfunctions of the middle vascular membrane are closely related to VSMC phenotypic conversion, transdifferentiation and apoptosis.^{6,7} Some studies have demonstrated that exosomes play an important role in angiogenesis, vascular calcification and senescence of VSMCs.⁸⁻¹¹ By transferring information among cells, exosomes in cellular senescence processes can regulate cell-cell communication.¹² However, whether exosomes are involved in the pathogenesis of vascular calcification and ageing remains unclear.

Melatonin (MT), secreted by the pineal gland, is a type of indole neuroendocrine hormone and necessary for holding physiological function.¹³ Many studies have shown that MT affects the cardiovascular system.¹⁴⁻¹⁶ It may play a role in protecting the heart by direct scavenging of free radicals and indirect antioxidant activity and by their obvious anti-inflammatory properties.¹⁷ Moreover, MT has been shown to antagonise premature senescence of cardiac progenitor cells (CPCs) via the H19/miR-675/USP10 pathway.¹⁸ However, the effect of MT on the osteogenic differentiation and senescence of VSMCs has not yet been elucidated.

Exosomes are small membrane particle containing RNAs, miRNAs and proteins. Its size ranges from 30 to 100 nm.¹⁹ Exosomes can carry miRNAs and thus affect recipient cell function, which suggests that the exosomal miRNAs play

an important role in intercellular communication.²⁰⁻²³ It has been reported that endothelial cells, which secrete exosomes containing miR-214, mediated the migration and angiogenesis of recipient endothelial cells, suggesting that cells secrete exosomes containing miRNAs to affect adjacent cells through a paracrine mechanism.²⁴ The mechanism involved in exosomal miRNA regulation of vascular calcification and senescence remains unclear. Therefore, this study aimed to characterise the effects of MT on calcification and ageing of arteries, and to investigate the regulatory role of exosomal miRNAs in this process.

2 | MATERIALS AND METHODS

2.1 | Ethics statement

All experiments were reviewed and approved by the Ethics Committee of the Second Xiang-Ya Hospital, Central South University. All the procedures conform to the Guide for the Care and Use of Laboratory Animals, NIH publication, 8th edition, 2011. All the animals were formally approved by the Ethics Committee of the Second Xiang-Ya Hospital, Central South University. The human samples conformed to the principles outlined in the Declaration of Helsinki. Human VSMCs were purchased from the National Platform of Experimental Cell Resources for SciTech (Beijing, China).

2.2 | Reagents

Dimethylsulphoxide (DMSO) (D2650), β -glycerophosphate (β -GP) (50020), PKH26 Red Fluorescent Cell Linker Kit (PKH26PCL), luzindole (L2407) and MT (M5250) were purchased from Sigma-Aldrich. DMEM/F12 (12634010) and foetal bovine serum (10099133C) were purchased from Gibco BRL Co. Lipofectamine 2000 (11668019) was purchased from Invitrogen Co. The antibody for β -actin (AM1021b, 1:1000) was purchased from Abgent Inc. Antibodies for MTNR1A (ab203038, 1:1000), MTNR1B (ab203346, 1:500), BMP2 (ab214821, 1:1000), p21 (ab218311, 1:1500), CD63 (ab134045, 1:5000), CD81 (ab59477, 1:1000), ALIX (ab186429, 1:5000), syntenin-1 (Synt1) (ab133267, 1:2000) and RUNX2 (ab23981,

1:1000) were purchased from Abcam. Maxima SYBR Green/ROX qPCR Master Mix (C0210B) and all of the primers used in this research were purchased from GeneCopoeia. The related secondary antibodies and the ECL detection kit (sc-2048) were purchased from Santa Cruz Biotechnology, Inc. BMP2 small interfering RNA (siRNA) oligos (siB0858163956-1-5) and control siRNA oligos were purchased from RiboBio. miR-204-5p/miR-211-5p mimics (miR10000265-1-5/miR10000268-1-5), inhibitors (miR20000265-1-5/miR20000268-1-5) and their control oligos were purchased from RiboBio. DAPI (C0065) was purchased from Solarbio. The alkaline phosphatase (ALP) kit (A059-1-1) was obtained from Jiancheng Nanjing Biological Engineering. The SA- β -gal kit (C0602) was purchased from Beyotime. The CCK8 assay kit (C008-3) was purchased from 7 Sea Biotech.

2.3 | Cell culture treatment and transfection

Vascular smooth muscle cells were maintained in DMEM:F12 medium supplemented with 10% foetal bovine serum and 1% penicillin/streptomycin (15070063, Gibco) at 37°C in 5% CO₂ infusion and humidified air. The medium was refreshed every 2 days. To induce calcification, the VSMCs were incubated with medium containing 10 mM β -GP. CVSMCs were obtained as described in our previous report.²⁵ CVSMCs were seeded in DMEM containing 4.5 g/L of glucose (21013024, Gibco), 10% FBS and 10 mM sodium pyruvate, and the medium was refreshed every 2 days. 10 μ M luzindole (Sigma-Aldrich) was added into the cultured VSMCs 2 hours before MT administration. At 12 hours after the onset of senescence, cells were treated with 10 μ M MT (Sigma-Aldrich) and vehicle for 48 hours. Total protein was extracted after 48 hours of treatment, and BMP2 and RUNX2 protein expression in VSMCs was analysed. miR-204-5p mimics were labelled with Label IT siRNA Tracker Cy5 Kit (MIR7213, MirusBio) according to the manufacturer's instructions. For transient transfection of BMP2 siRNA oligos, a combination of oligos (50 nM) and Lipofectamine 2000 was mixed according to the manufacturer's instructions and added to cells in 6-well plates at a density of 2×10^5 cells per well.

2.4 | Exosome isolation and purification

Using differential centrifugation, exosomes were isolated and purified from the supernatants of VSMC cultures. The VSMC were cultured in DMEM/F12-containing exosome-depleted serum. CVSMCs were cultured in DMEM-containing exosome-depleted serum. After treatment with MT for 48 hours, the medium was collected and centrifuged

at 2000 g for 15 minutes at 4°C and centrifuged again at 12 000 g for 45 minutes at 4°C. Then, the supernatants were passed through a 0.22-mm filter (Millipore) and ultracentrifuged at 110 000 g for 90 minutes at 4°C. The pellets were washed with PBS followed by a second ultracentrifugation at 110 000 g for 90 minutes at 4°C and resuspended in PBS. The BCA Protein Assay Kit (23225, Pierce) was used to measure the protein levels of the exosomes according to the manufacturer's instruction.

2.5 | Identification of exosomes

The pelleted exosomes were resuspended in approximately 100 mL of PBS and subjected to transmission electron microscopy (Hitachi H-7650, Hitachi) for morphology analysis and Nanosight 2000 analysis (Particle Metrix) for diameter analysis. Exosomal marker proteins, including CD63, CD81, ALIX and Synt1, were analysed using Western blot. The PKH26 Red Fluorescent Cell Linker Kit was used to observe exosomes uptake according to the manufacturer's instructions.

2.6 | Western blot analysis

Western blot analysis was carried out for the detection of MTNR1A, MTNR1B BMP2, RUNX2, p21, CD63, CD81, ALIX, Synt1 and β -actin protein levels as previously described. Sodium dodecyl sulphate-polyacrylamide gel electrophoresis was used to analyse 30 μ g of protein from each cell layer extract and then transferred to a polyvinylidene fluoride membrane. The membrane, after blocking with 5% nonfat milk, was incubated with MTNR1A, MTNR1B, BMP2, p21, RUNX2, CD63, CD83, ALIX, Synt1 and β -actin antibodies overnight at 4°C. The following morning, the membrane was washed with PBS three times every 10 minutes. The membrane was then incubated with appropriate secondary antibody (1:2000 dilution) in 2% nonfat milk for 1 hour. Blots were processed using an enhanced chemiluminescence (ECL) kit, exposed to film and analysed by densitometry.

2.7 | Measurement of osteogenesis differentiation of VSMCs

After being subjected to different treatments, the VSMCs were washed with PBS and scraped into solution. Spectrophotometric measurement of p-nitrophenol released at 37°C was utilised to analyse ALP activity. ALP activity was normalised by total protein content of the cell lysate.

Name	Primers
WT BMP2	5' GGGTTTAAACGGATAACCCGAGATAAAG 3' 5' GCTCTAGACAATCTGAGCAGCCTAAT 3'
Mut BMP2	5' CGGTGCCAGAAAATTAGAGCGCAAAGTGTCGG 3' 5' CCGACACTTTGCCGCTCTAATTTTCTGGCACCG 3'

TABLE 1 Nucleotide sequences of primers for construct and mutation of plasmids

Calcification was visualised following fixation with 4% formaldehyde for 15 minutes and staining with Alizarin Red S (2%, pH 4.2), as previously described.²⁶ To determine the calcium content, Alizarin Red S stain released from the cell matrix was quantified by incubation in cetylpyridinium chloride and measured using spectrophotometry at 540 nm. The calcium quantities were normalised to total cellular protein. The results were compared with the control and presented as the fold change using data from three independent experiments.

2.8 | Gene expression estimated using qRT-PCR

Total RNA was extracted from exosomes and VSMCs, and cDNA was prepared. For analysis of miR-204-5p/miR-211-5p expression, reverse transcription and quantitative reverse transcription-polymerase chain reaction (qRT-PCR) was carried out using the primer for miR-204-5p/miR-211-5p (GeneCopoeia, HmiRQP0306/ HmiRQP0318) according to the manufacturer's instructions. Relative quantification was calculated using the $2^{-\Delta\Delta CT}$ method. U6 levels (for cellular miR-204-5p/miR-211-5p) or miR-16 (for exosomal miR-204-5p/miR-211-5p) was used to normalise data.²⁷

2.9 | SA- β -gal assay

According to the manufacturer's instructions, senescence-associated- β -galactosidase (SA- β -gal) staining was performed using a SA- β -gal staining kit (C0602, Beyotime). Digital images in 10 randomly chosen fields were viewed and analysed with an image analysis program (BioQuant), and each sample was counted to calculate the percentage of senescent cells to quantify the percentage of SA- β -gal-positive cells.

2.10 | Cell growth assay

The growth and viability of VSMCs were determined by the cell counting kit 8 (CCK8) assay. At a density of 1500 cells per well in growth medium, VSMCs were seeded into 96-well tissue culture plates. The cells were washed twice with PBS after treatment. Using the CCK8 assay with absorbance

measured at 450 nm, the cell number was determined. The assay was repeated three times.

2.11 | Transwell assay

We placed Transwell assay inserts (Corning, NY, USA) into a 6-well plate. In the experiment, VSMCs (4×10^5 cells/well) were first treated with GW4869 (S7609) or vehicle in the bottom chamber incubated with 10 μ M MT and DMEM/F12-containing exosome-depleted serum culture medium was added to the bottom chamber for 48 hours. Then, VSMCs attached to the upper surface of the filter membranes without treatment were used to analyse osteogenic differentiation and senescence of VSMCs.

2.12 | Plasmid constructs and luciferase reporter assay

To analyse the function of miR-204-5p/miR-211-5p, segments of the BMP2 3'-UTR, including the predicted miR-204-5p/miR-211-5p binding sites, were cloned into the PmeI and XbaI restriction sites of the luciferase reporter vector pmirGLO (E1330, Promega) producing wild-type BMP2 3'-UTR (WT-BMP2-3'-UTR). The BMP2 mutants for the miR-204-5p/miR-211-5p seed regions were produced using the QuikChange Site-Directed Mutagenesis Kit (210518, Stratagene) to obtain mutant BMP2 3'-UTR (MUT-BMP2-3'-UTR).

Vascular smooth muscle cells were cotransfected with a luciferase reporter carrying WT-BMP2-3'-UTR or MUT-BMP2-3'-UTR and miR-204-5p/miR-211-5p mimics or control. Sequences of the PCR and mutagenic primers are shown in Table 1. At 48 hours after transfection, luciferase activities were detected with the luciferase assay system (Promega). Firefly luciferase activity was normalised to the corresponding Renilla luciferase activity. Luciferase assays were performed in quadruplicate and repeated in three independent experiments.

2.13 | Animals' studies

Mice were fed with 12-hour daylight/darkness transition in Animal House of the Second Xiang-Ya Hospital. To generate

vascular calcification and ageing in mice, the 5/6 NTP mouse model was established following the procedure previously described.²⁸ Briefly, 6-week-old C57BL/6 mice were treated with an intraperitoneal injection of pentobarbital sodium (50 mg/kg) to induce general anaesthesia before operation. The anaesthesia state of the mice was validated frequently by loss of the pedal withdrawal reflex. Firstly, the upper and lower poles of left side kidney were removed with the adrenal gland reserved. Two weeks later, the right side of kidney was fully removed. Sham control mice were subjected to the same surgery at the same time as the 5/6 NT group, with exposure of the kidney. But only removal of the renal capsule instead of the kidney tissue was performed in sham mice, and then, the abdomen skin was closed. Subsequently, a high-phosphate diet (0.9% Pi) was used to accelerate calcification throughout the study. The successful setup of the mouse model was confirmed by increasing level of serum urea nitrogen and creatinine.

In some specific experiments, MT dissolved in 0.1% DMSO and diluted by saline solutions) was given via intraperitoneal (*i.p.*) injection at the concentration of 20 mg/kg every day before darkness for 4 weeks (1 week after the last operation).²⁹ Circulating exosomes were inhibited by GW4869 (*i.p.*, 2 mg/kg) every 2 days throughout the study as reported previously.³⁰ After the treatment, mouse thoracic aorta was isolated free of adventitia, and blood samples were collected.

2.14 | Immunohistochemistry

The expression of p21(ab218311, 1:150) and RUNX2 (ab76956, 1:100) in the aorta tissue was examined by immunohistochemistry in a similar method as reported previously.³¹ Briefly, the thoracic aorta was fixed in 4% paraformaldehyde overnight, then embedded in paraffin and cut into 5- μ m sections. Subsequently, sections were incubated at 65°C in the oven for 2 hours, followed by two dewaxings in xylenes at 10 minutes of intervals and then dehydrating in 99%, 95% and 75% ethanol for 5 minutes. Citrate was used for antigen retrieval at boiling temperature for 20 minutes, and hydrogen peroxide incubation was performed at room temperature in a dark box for 10 minutes to diminish endogenous peroxidases. Sections were then blocked by 5% foetal serum for an hour, followed by incubating with a specific primary antibody overnight with rocking at 4°C. The next day, sections were rewarmed at room temperature for 30 minutes and then incubated with a secondary antibody for 30 minutes at room temperature. A DAB kit was used to detect positive staining. Finally, sections were counterstained with haematoxylin. Photographs were used for analysis by Image-Pro Plus software (version 6.0).

2.15 | Von Kossa staining, Alizarin Red S staining and detection of ALP activity and calcium content of the thoracic aorta

Vascular calcification in mice was detected by Von Kossa staining and Alizarin Red S (0.5%, pH 9.0, Sigma) staining in a similar way that was described previously.³² Briefly, sections were dewaxed in xylene and dehydrated in alcohol as described previously. For Alizarin Red S staining, sections were washed by PBS and incubated by Alizarin Red S (0.5%, pH 9.0, Sigma) 30-60 seconds at 37°C. For Von Kossa staining, sections were incubated by silver nitrate (5%, Sigma) 1 hour under exposure of the ultraviolet light, following by incubation in sodium thiosulfate for 10 minutes. Photomicrographs were used for analysed by Image-Pro Plus software (version 6.0) to detect positive staining area.

Measurement of the ALP activity was performed in a similar way as described in previous article.^{33,34} The o-cresolphthalein complexone method was performed to measure the calcium content as previously described.³⁵ Briefly, dried artery samples were incubated and decalcified with HCl at room temperature. The calcium content in HCL dissolved supernatants was then analysed using the o-cresolphthalein method. Total protein was detected using the Bradford protein assay. The calcium content was normalised with protein content and presented as microgram calcium/milligram protein.

2.16 | Vascular SA- β -gal staining and immunofluorescence

To identify senescence and detect specific proteins in the thoracic aorta, mouse aorta tissues were isolated on ice dry, immediately stored in liquid nitrogen and mounted in OCT. Tissues were cut into 5- μ m frozen sections and then used for SA- β -gal staining and immunofluorescence.

SA- β -gal staining was performed similarly to the procedure as described by Hu et al³⁶ Briefly, aortic sections were fixed in PBS containing 2% formaldehyde and 0.2% glutaraldehyde for 5 minutes and then incubated with SA- β -gal staining solution for 18 hours at 37°C. Subsequently, aortic sections were counterstained with Nuclear Fast Red.

For double staining, frozen sections of aorta were incubated with the rat exosome marker TSG101 monoclonal antibody (ab125011, 1:100) and VSMC mouse marker α SMA monoclonal antibody (GB13044, 1:500) followed by detection with Cy3-conjugated goat anti-rabbit IgG (GB21303, 1:300) and Alexa Fluor[®]488-conjugated goat anti-mouse IgG (GB25301, 1:400). Sections were examined by fluorescence confocal microscope (Nikon).

2.17 | In vivo tracking of exosomes and exosome injection

To label exosomes, 1,1'-dioctadecyl-3,3,3',3'-tetramethylindotricarbocyanine iodide (DiR; 2024243, Thermo Fisher Scientific/Invitrogen), diluted in ethanol at a concentration of 1 mg/mL, was mixed with exosomes at the ratio of 2 µg DiR/100 µg exosomes in PBS for 1 hour followed by ultracentrifugation at a speed of 100 000 g for 1 hour to remove unincorporated DiR and ethanol. The precipitate was resuspended in PBS at a concentration of 1 µg exosome/1 µL PBS. PBS vehicle, DiR or DiR-labelled exosome was injected via the tail vein, and an in vivo fluorescence image was taken 24 hours later using Ami X spectral imaging instrument and analysed by in vivo imaging software.

Given the physiological amount of circulating exosomes in mice, a previous study has shown that tail vein injections of 100 µg exosomes every 3 days were suitable for an in vivo study based on a mouse model.³⁷ In the present study, we treated 5/6 NTP-induced C57BL/6J mice with 100 µg exosomes that derived from vehicle (VSMCs^{veh}-exo) or MT-treated VSMCs (VSMCs^{MT}-exo) respectively, via tail vein injections at an interval of 3 days for 4 weeks (nine injections total). Blood samples and aortic tissues were harvested, and frozen sections of aortic tissues were used for the detection of the exosome marker TSG101 to identify uptake of VSMCs-exos by mouse VSMCs.

2.18 | Statistical analysis

The results of the experiments are presented as means ± SD, and analysis was performed with Statistical Product and Service Solutions (SPSS) software (version 19.0). Comparisons between values of more than two groups were evaluated by an analysis of variance (one-way ANOVA). A level of $P < .05$ was considered statistically significant. All experiments were repeated at least three times. Figures show the representative experiments.

3 | RESULTS

3.1 | Melatonin can antagonise VSMC osteogenic differentiation and senescence via a MT membrane receptor-dependent manner

To investigate the effect of MT on the role of osteogenic differentiation and senescence of VSMCs, VSMCs were treated with different concentrations of MT (10 nM, 100 nM, 1 µM, 10 µM and 100 µM). As shown in Figure 1, we found that 10 µM MT had the greatest effect on attenuating the osteogenic differentiation and senescence of VSMCs (Figure 1A-C). Western

blot analysis revealed that the expression of RUNX2 was inhibited by MT in a concentration-dependent manner (Figure 1A). Moreover, MT could also attenuate β-GP-induced ALP activity and senescence in a concentration-dependent manner (Figure 1B,C). The osteogenic differentiation of VSMCs was suppressed after 10 µM MT treatment as shown by the protein expression of RUNX2, ALP activity, Alizarin Red staining and calcium content (Figure 1D-F). In addition, the senescence of VSMCs was attenuated by 10 µM MT as shown by decreased p21 expression, SA-β-gal staining (Figure 1D,G) and increased proliferation of VSMCs as evidenced by the CCK8 assay (Figure 1H). These data suggest that MT could attenuate osteogenic differentiation and senescence of VSMCs.

We also investigated whether MT could attenuate osteogenic differentiation and senescence of VSMCs via an MT membrane receptor-dependent manner. The expression of MTNR1A and MTNR1B, the MT membrane receptor, both expressed in VSMCs and CVSMCs as demonstrated by Figure S1A and Figure S1B. As shown in Figure 1D, the effect of MT on decreasing the expression of RUNX2 and p21 of VSMCs was blocked by the presence of 10 µM luzindole, an MT membrane receptor blocker. Likewise, the inhibitory effects of MT on osteogenic differentiation and senescence of VSMCs were also attenuated by luzindole (Figure 1D-H). These results suggest that the MT membrane receptor is involved in MT attenuating VSMC osteogenic differentiation and senescence.

3.2 | VSMC-derived exosomes induced by MT inhibit VSMC calcification and senescence

To analyse whether the exosomes secreted by VSMCs play a role in the MT-induced attenuation effect of osteogenic differentiation and senescence of VSMCs, we isolated exosomes from VSMCs. Transmission electron microscopy and Nanosight analysis were used to characterise the VSMC-derived nanoparticles. As shown in Figure 2A, these vesicles exhibited a typical cup or sphere-shaped morphology. Nanosight analysis showed that the size of most of VSMCs exosomes (VSMCs-Exos) was approximately 80-140 nm (Figure 2B). Western blotting revealed that the exosome marker proteins CD63, CD81, ALIX and Synt1 were strongly enriched in VSMCs-exos compared with the cell lysis (Figure 2C). These results confirmed that these vesicles were exosomes.

To further investigate whether VSMCs-exos could exhibit a paracrine effect on VSMCs, we examined whether these exosomes could be taken up by VSMCs. We labelled VSMC-derived exosomes with PKH26 (a red fluorescent cell linker dye with a long aliphatic carbon tail) and incubated VSMCs with the labelled exosomes. Confocal microscopy analysis showed that the labelled exosomes were taken up by the VSMCs (Figure 2D). To demonstrate whether MT can antagonise osteogenic differentiation and senescence of VSMCs via exosomes, we treated

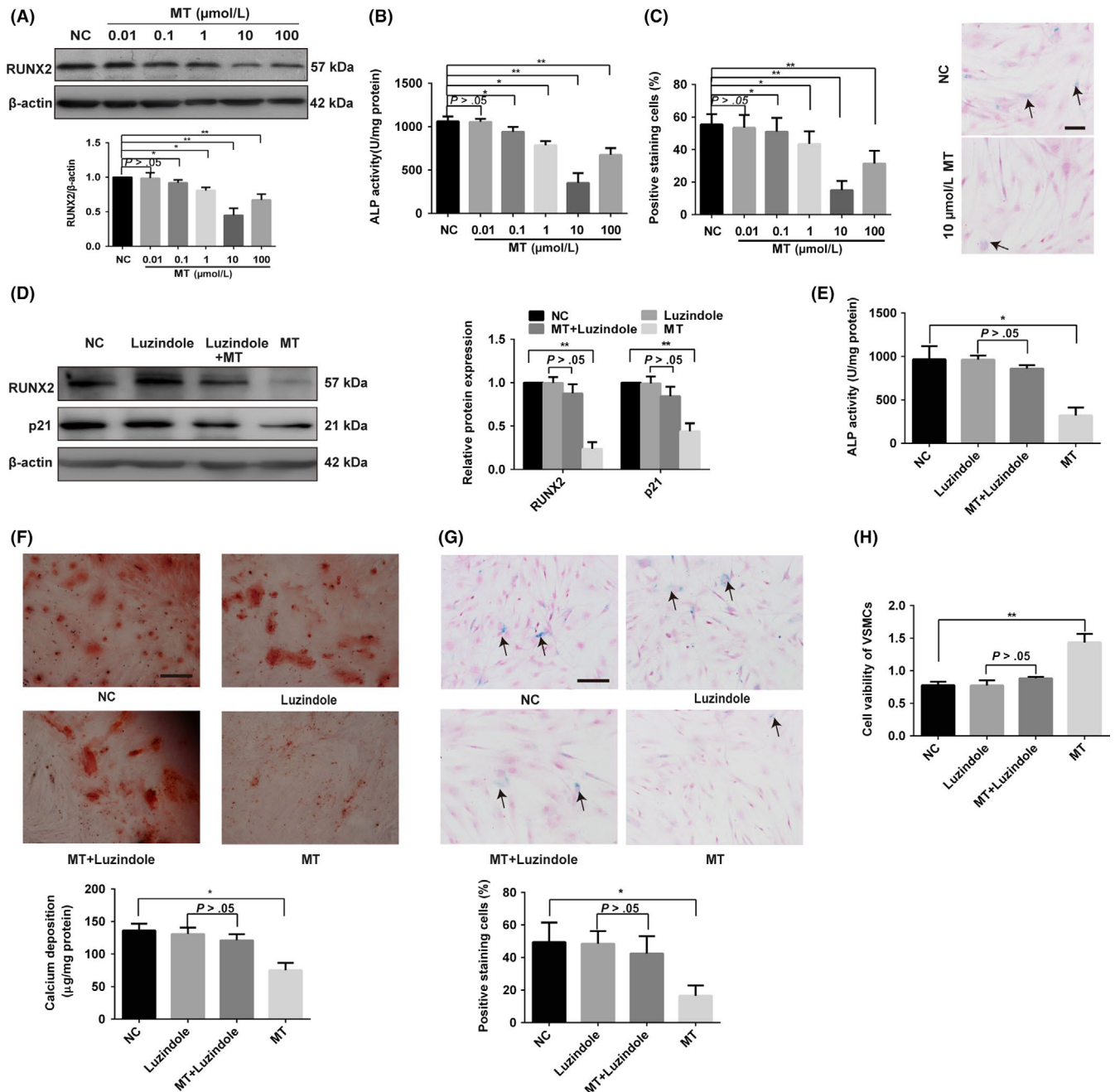


FIGURE 1 Melatonin can antagonise VSMC osteogenic differentiation and senescence via an MT membrane receptor-dependent manner. A-C, Effects of melatonin (MT) on RUNX2 expression, ALP activity and senescence level. VSMCs were treated with 10 mM β -glycerophosphate (β -GP) and different concentrations of MT (10 nM, 100 nM, 1 μ M, 10 μ M and 100 μ M) or vehicle for the control. A, The expression of RUNX2 was determined by Western blotting. B, ALP activity was measured using an ALP kit, normalised to the cellular protein content. C, SA- β -gal staining was performed to detect cell senescence level. Semi-quantitative analysis of SA- β -gal-positive cells (left panel) and representative microphotographs (right panel) are shown. D, The protein levels of RUNX2 and p21 were determined by Western blotting in vehicle, luzindole, 10 μ M MT plus luzindole or 10 μ M MT-treated VSMCs. E, ALP activity assays were measured using an ALP kit for vehicle, luzindole, 10 μ M MT plus luzindole or 10 μ M MT-treated VSMCs. F, β -GP-induced VSMCs were treated with vehicle, luzindole, 10 μ M MT plus luzindole or 10 μ M MT for 14 days and then subjected to Alizarin Red S staining. Calcium deposition was extracted with cetylpyridinium chloride and quantified by spectrophotometry. G, VSMCs were treated with vehicle, luzindole, 10 μ M MT or 10 μ M plus luzindole and then subjected to SA- β -gal staining. Semi-quantitative analysis of SA- β -gal-positive cells was performed. Representative microscopic views are shown. Scale bar represents 200 μ m. H, CCK8 assay was performed in VSMCs treated with vehicle, luzindole, 10 μ M MT plus luzindole or 10 μ M MT. The data represent the mean \pm SD. NC, normal control. * $P < .05$, ** $P < .01$

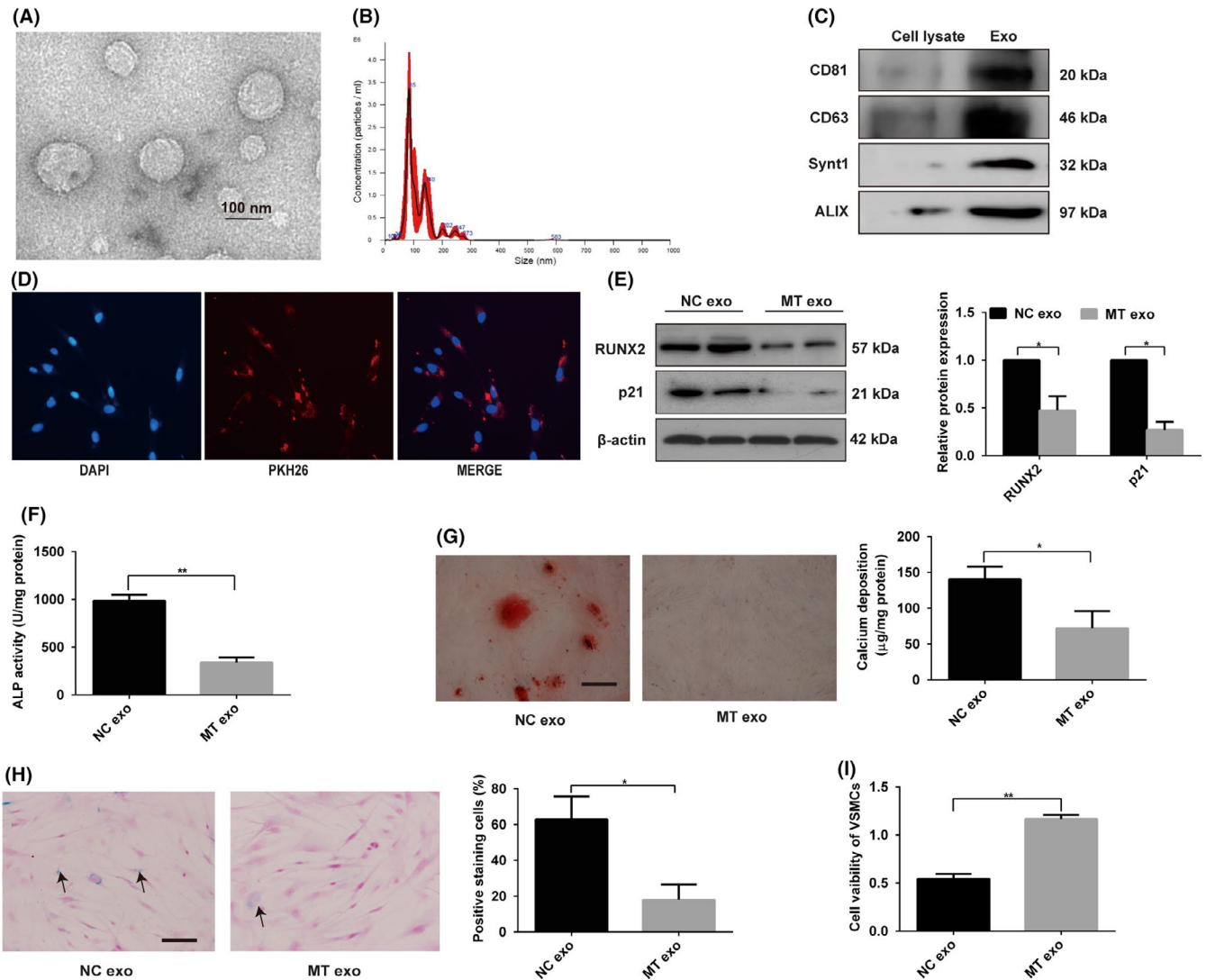


FIGURE 2 VSMC-derived exosomes induced by MT inhibit VSMC calcification and senescence. A, Transmission electron microscopic analysis of exosomes is shown. Scale bar represents 100 nm. B, Nanoparticle tracking analysis of exosomes derived from VSMCs showed that the size of most of VSMC-exos was approximately 80-140 nm. C, Western blotting showed exosome-specific proteins CD81, CD63, Synt-1 and ALIX were abundant in exosomes compared with cell lysate. D, VSMCs incubated with PKH26 fluorescently labelled exosomes for 12 h. Confocal microscopy analyses used to identify the uptake of exosomes by VSMCs are shown (PKH26 in red, DAPI in blue). Magnification, 100 \times . E, The expression of RUNX2 and p21 was determined by Western blotting in VSMCs incubated with exosomes from MT-treated VSMCs or exosomes from vehicle-treated VSMCs. F, ALP activity was determined by an ALP kit in VSMCs incubated with exosomes from MT-treated VSMCs or exosomes from vehicle-treated VSMCs. G, Alizarin Red S staining and calcium content were measured in VSMCs incubated with exosomes from MT-treated VSMCs or exosomes from vehicle-treated VSMCs. Representative microscopic views are shown. Scale bar represents 200 μ m. H, VSMCs incubated with exosomes from MT-treated VSMCs or exosomes from vehicle-treated VSMCs and then subjected to SA- β -gal staining. Semi-quantitative analyses of SA- β -gal-positive cells were performed. Representative microscopic views are shown. Scale bar represents 200 μ m. I, CCK8 assays were performed in VSMCs incubated with exosomes from MT-treated VSMCs or exosomes from vehicle-treated VSMC. Three independent experiments were performed, and representative data are shown. Data are shown as mean \pm SD. * P < .05, ** P < .01, compared with normal control

VSMCs or CVSMCs with exosomes isolated from VSMCs or CVSMCs incubated with MT, respectively. These exosomes significantly inhibited osteogenic differentiation, as evident by the decreased protein level of RUNX2 (Figure 2E and Figure S2A), ALP activity (Figure 2F and Figure S2B), Alizarin Red staining and calcium content (Figure 2G and Figure S2C). Moreover, the exosomes isolated from MT-treated VSMCs may suppress

senescence of VSMCs, as demonstrated by the reduced protein level of p21 (Figure 2E and Figure S2A), fewer SA- β -gal-positive VSMCs (Figure 2H and Figure S2D) and induced proliferation of VSMCs as evident by CCK8 assay (Figure 2I and Figure S2E). These data clearly indicate that the exosomes secreted by MT-treated VSMCs or CVSMCs could antagonise the osteogenic differentiation and senescence of VSMCs or CVSMCs, respectively.

3.3 | MT attenuated the calcification and senescence of VSMCs by affecting exosomes in a paracrine manner

To further identify the role that exosomes play in the paracrine effect on the osteogenic differentiation and senescence of VSMCs, we treated VSMCs with fresh conditional medium (control), whole MT-treated VSMCs conditional medium (MT-VSMCs-CM) or MT-treated VSMCs exosome-free conditional medium (MT-VSMCs-exo-free-CM) to analyse whether exosomes could mediate the effect of MT on VSMCs. Our results indicated that MT-VSMCs-CM could attenuate the osteogenic differentiation and senescence of VSMCs when compared with the control group (Figure 3A-C), which showed a similar effect of exosomes isolated from MT-treated VSMCs. By contrast, MT-VSMCs-exo-free-CM could not decrease the osteogenic differentiation and senescence of VSMCs when compared with the control group (Figure 3A-C). To further analyse the effect of exosomes on the osteogenic differentiation and senescence of VSMCs, VSMCs were pretreated with the noncompetitive N-SMase inhibitor GW4869, an inhibitor of exosome secretion, to block exosome secretion. The inhibition effects of MT-VSMCs-CM on VSMC osteogenic differentiation and senescence were abolished after treatment of GW4869 (Figure 3A-C). These data clearly indicate that the exosomes secreted from MT-treated VSMCs could decrease VSMC osteogenic differentiation and senescence. By contrast, exosome-depleted culture medium from MT-treated VSMCs and VSMCs with impaired exo-producing function had little effect on VSMC osteogenic differentiation and senescence, which suggested MT could attenuate the osteogenic differentiation and senescence of VSMCs by affecting exosomes in a paracrine manner.

To analyse the paracrine effect of VSMCs through exosomes, we cocultured VSMCs in a Transwell system. In this system, VSMCs in the lower chamber incubated with MT and treated with or without GW4869 were cocultured with VSMCs in the upper chamber, respectively. RUNX2 expression and ALP activity were decreased in the VSMCs in the upper chamber in the MT plus vehicle-treated group compared with the MT plus GW4869-treated group (Figure 3D-F). Meanwhile, the expression of p21 was decreased in MT plus vehicle-treated group compared with MT plus GW4869-treated group (Figure 3E), and the proliferation of VSMCs was increased in MT plus vehicle-treated group compared with MT plus GW4869-treated group as evident by CCK8 assay (Figure 3G). These data confirmed that exosomes secreted by MT-treated VSMCs could attenuate the osteogenic differentiation and senescence of VSMCs while blocking the exosome secretion attenuated the paracrine effect of MT on VSMCs.

3.4 | MT induced exosomal miR-204 and miR-211 antagonise VSMC osteogenic differentiation and senescence

Previous studies have suggested that miRNAs play a pivotal role in vascular calcification.⁴ We detected eight miRNAs related to calcification in exosomes secreted by VSMCs treated with or without MT by qRT-PCR. Our results showed that the expression of miR-204 and miR-211, both in VSMCs and exosomes, was significantly upregulated by MT treatment compared with control (Figure 4A,B). These results indicate that MT induced significant upregulation of miR-204 and miR-211 both in VSMCs and exosomes secreted by VSMCs.

Some studies have demonstrated that miR-204 and miR-211 play a key role in vascular calcification.^{4,35} We hypothesised that exosomal miR-204 and miR-211 participated in the process of vascular osteogenic differentiation and senescence by a paracrine mechanism. To further confirm that miR-204 and miR-211 antagonise VSMC osteogenic differentiation and senescence, we transfected miR-204 and miR-211 mimics into VSMCs. As shown in Figure 4C, both miR-204 and miR-211 were significantly upregulated in exosomes. To verify exosomal miR-204 and miR-211 could be uptaken by VSMCs, we used FAM-miR-204 mimics as an example. VSMCs were cultured with PKH26-labelled exosomes derived from VSMCs transfected with FAM-miR-204-mimics; then, the FAM-miR-204 signals were detected in the cytoplasm of VSMCs (green). FAM-miR-204 signals were co-localised with PKH26 in VSMCs (PKH26 in red, DAPI in blue; Figure 4D), which suggested that exosomal miR-204 could be uptaken by VSMCs. Moreover, exosomes from VSMCs transfected with miR-204/miR-211 mimics for 48 hours exhibited reduced RUNX2 expression (Figure 4E) and ALP activity (Figure 4F). Senescence of VSMCs was also decreased confirmed by reduced p21 expression (Figure 4E), fewer SA- β -gal-positive VSMCs and induction of VSMC proliferation (Figure 4G, H). Thus, we verified that MT could induce exosomal miR-204 and miR-211 to attenuated VSMC osteogenic differentiation and senescence via exosomes.

3.5 | BMP2 is the direct target gene of miR-204 and miR-211

By binding to the 3' UTR region of downstream target genes, miRNAs regulate their target gene expression. We used several bioinformatic target prediction algorithms to search for targets of miR-204 and miR-211. BMP2 was predicted to be a potential target of miR-204 and miR-211 (Figure 5A). To clarify whether miR-204 or miR-211 can directly bind to the 3' UTR of BMP2, luciferase reporter constructs containing unaltered or mutated predicted miRNA-binding sites of BMP2 (WT-pGL3-BMP2 and MUT-pGL3-BMP2, respectively) were constructed. Table

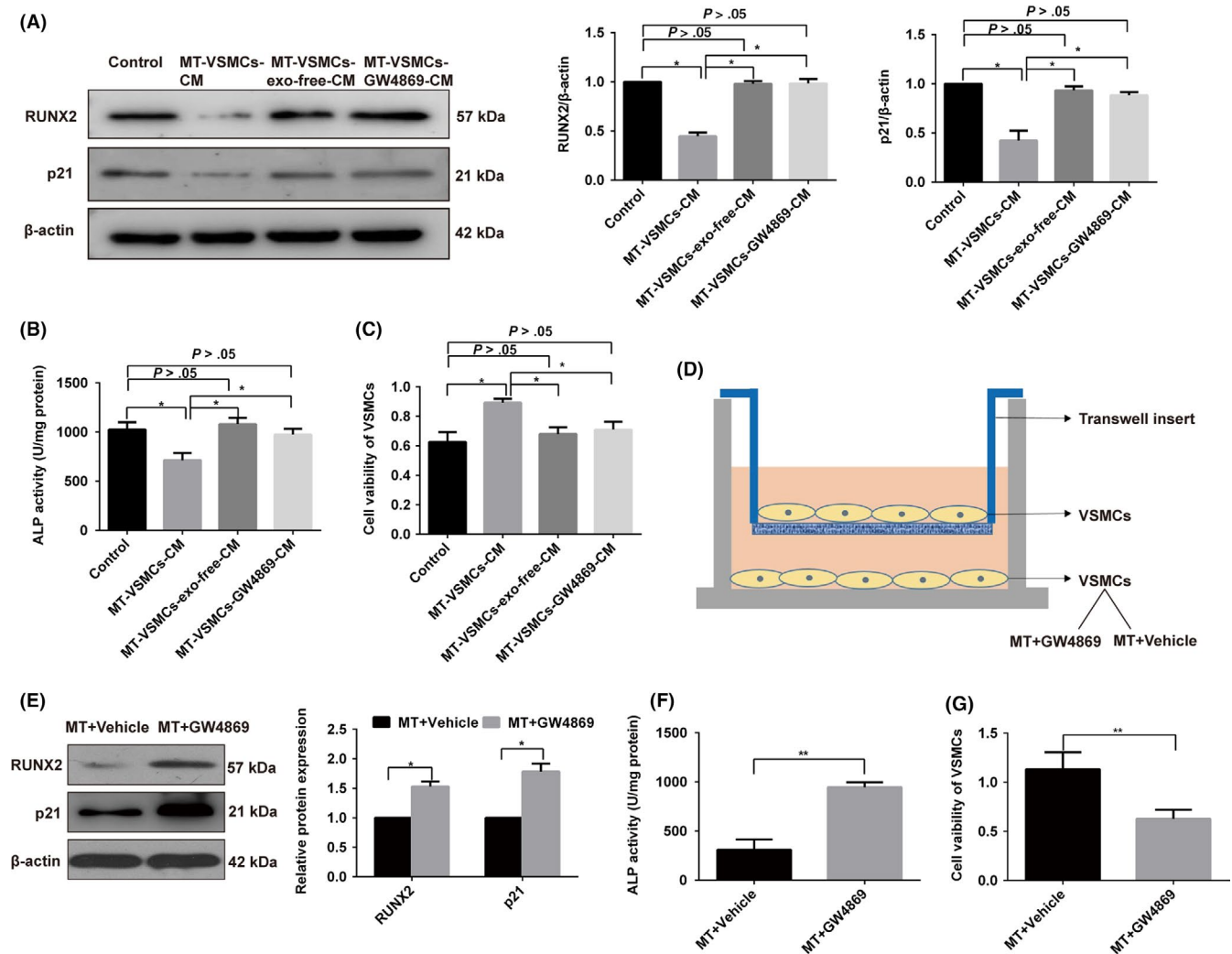


FIGURE 3 MT attenuated the calcification and senescence of VSMCs by affecting exosomes in a paracrine manner. VSMCs were treated with fresh conditional medium (control), whole MT-treated VSMCs conditional medium (MT-VSMCs-CM), MT-treated VSMCs exosome-free conditional medium (MT-VSMCs-exo-free-CM) or MT-treated VSMCs exosome with GW4869 conditional medium (MT-VSMCs-GW4869-CM), respectively. All groups were incubated with β-GP at the same time. A, The protein levels of RUNX2 and p21 were determined by Western blotting. B, ALP activity assays were determined with an ALP measurement kit. C, CCK8 assay was performed to detect cell proliferation. D, Schematic representation of coculture Transwell system to analyse the exosomal paracrine effects of VSMCs. VSMCs in lower chamber incubated with MT and treated with or without GW4869 were cocultured with VSMCs without treatment in the upper chamber in six-well Transwell units. And the upper chamber VSMCs were used to determine the expression of RUXN2, p21, ALP activities and cell viability. E, Western blotting showed that RUNX2 and p21 increased in the VSMCs from the upper chamber in MT plus GW4869 group compared with MT plus vehicle. F, ALP activity assays showed that MT plus GW4869 group had higher ALP activity compared with MT plus vehicle. G, CCK8 assay showed that MT plus GW4869 treatment decreased the proliferation of senescence VSMCs compared with MT plus vehicle. Three independent experiments were performed, and representative data are shown. The data represent the mean \pm SD. NC, normal control. $*P < .05$, $**P < .01$

1 showed the sequences of the PCR and mutagenic primers. We transfected WT-pGL3-BMP2 and MUT-pGL3-BMP2 with miR-204 or miR-211 mimics into VSMCs and measured the effects of miR-204 or miR-211 on luciferase enzyme activity. miR-204 and miR-211 mimics repressed the luciferase activity of the BMP2 3'-UTR reporter gene, while MUT-pGL3-BMP2 abolished this inhibition (Figure 5B). These data demonstrate that miR-204 and miR-211 directly target the 3' UTR of BMP2. Furthermore, our results reveal that the overexpression of miR-204 or miR-211 in VSMCs could decrease, while inhibition of

miR-204 or miR-211 could promote the endogenous expression of BMP2 in VSMCs (Figure 5C).

3.6 | Osteogenic differentiation and senescence of VSMCs is associated with BMP2

BMP2 is reported to be involved in age-related vascular calcification. Thus, we investigated whether BMP2 is involved in osteogenic differentiation and senescence of VSMCs. Our

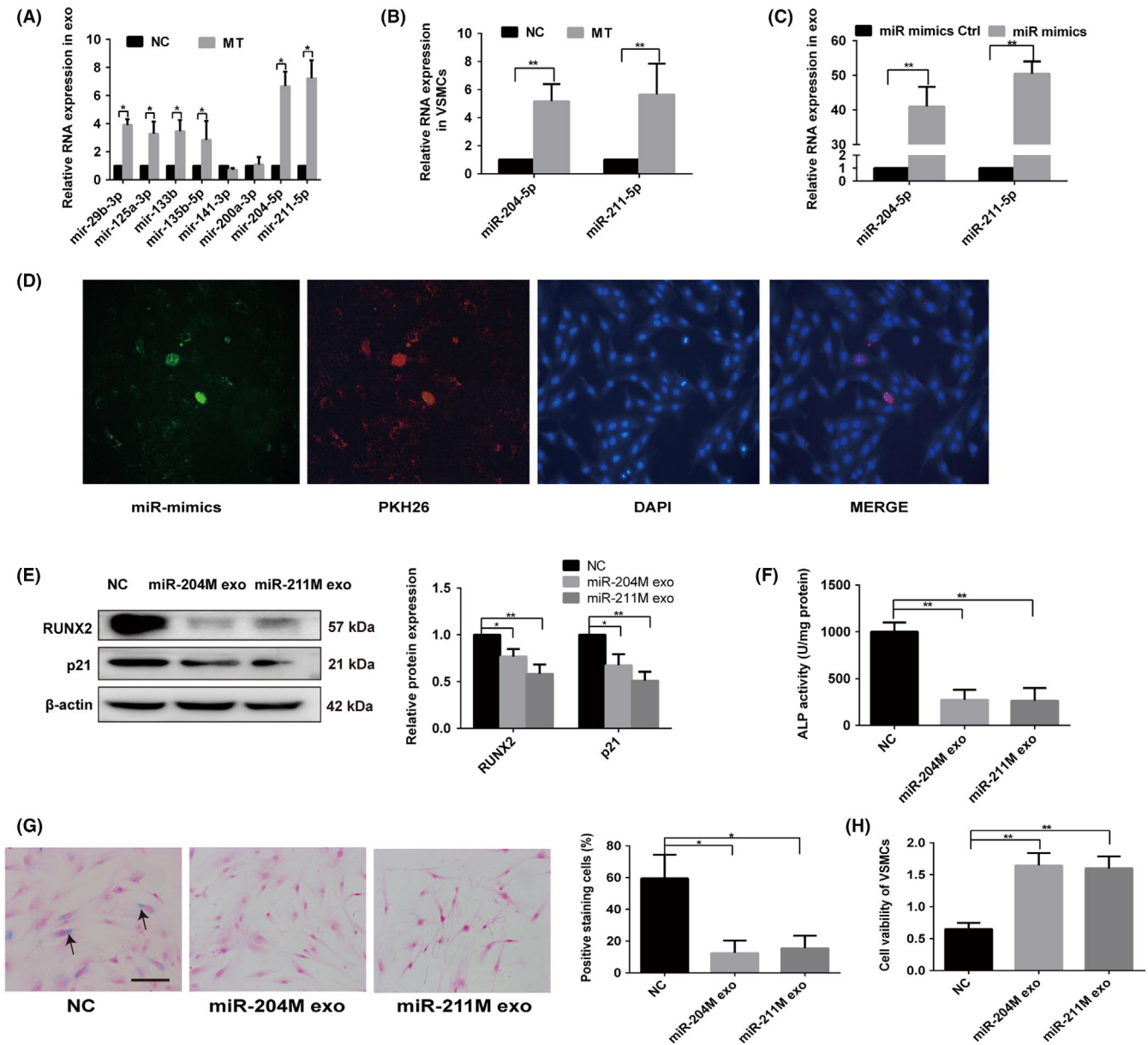


FIGURE 4 MT induced exosomal miR-204 and miR-211 antagonise VSMC osteogenic differentiation and senescence. A, qRT-PCR analysis of eight microRNAs in exosomes derived from MT-treated VSMCs or vehicle-treated VSMCs. B, qRT-PCR analysis of miR-204 and miR-211 expression in VSMCs treated with MT or vehicle. C, qRT-PCR analysis of miR-204 and miR-211 in VSMCs after miR-204/211 mimics or mimics control transfection. D, Confocal microscopy analysis was used to verify exosomal miR-204 could be uptaken by VSMCs. VSMCs were cultured with PKH26-labelled exosomes derived from VSMCs transfected FAM-miR-204-mimics. The FAM-miR-204 signals were detected in the cytoplasm of VSMCs (Green), and FAM-miR-204 signals were co-localised with PKH26 in VSMCs (PKH26 in red, DAPI in blue). Magnification, 100 \times . E, The expression of RUNX2 and p21 was determined with Western blotting in VSMCs treated with exosomes from miR-204/211 overexpression VSMCs or exosomes from mimic control transfected VSMCs. F, ALP activity was determined using an ALP kit in VSMCs treated with exosomes from miR-204/211 overexpression VSMCs or exosomes from mimic control transfected VSMCs. G, VSMCs treated with exosomes from miR-204/211 overexpression VSMCs or exosomes from mimic control transfected VSMCs and then subjected to SA- β -gal staining. Semi-quantitative analyses of SA- β -gal-positive cells were performed. Representative microscopic views are shown. Scale bar represents 200 μ m. H, CCK8 assays were performed in VSMCs treated with exosomes from miR-204/211 overexpression VSMCs or exosomes from mimic control transfected VSMCs. Three independent experiments were performed, and representative data are shown. NC, normal control. * P < .05. ** P < .01. NC, normal control

results showed the effect of BMP2 knockdown by siRNA in VSMCs. Western blot analysis confirmed that BMP2 was significantly downregulated (Figure 5D). As expected, the expression of RUNX2 and p21 was significantly downregulated

following transfection with BMP2 siRNA for 48 hours (Figure 5D); ALP activity was also reduced (Figure 5E). Moreover, CCK8 assay analysis indicated that downregulation of BMP2 induced proliferation of VSMCs (Figure 5F). SA- β -gal

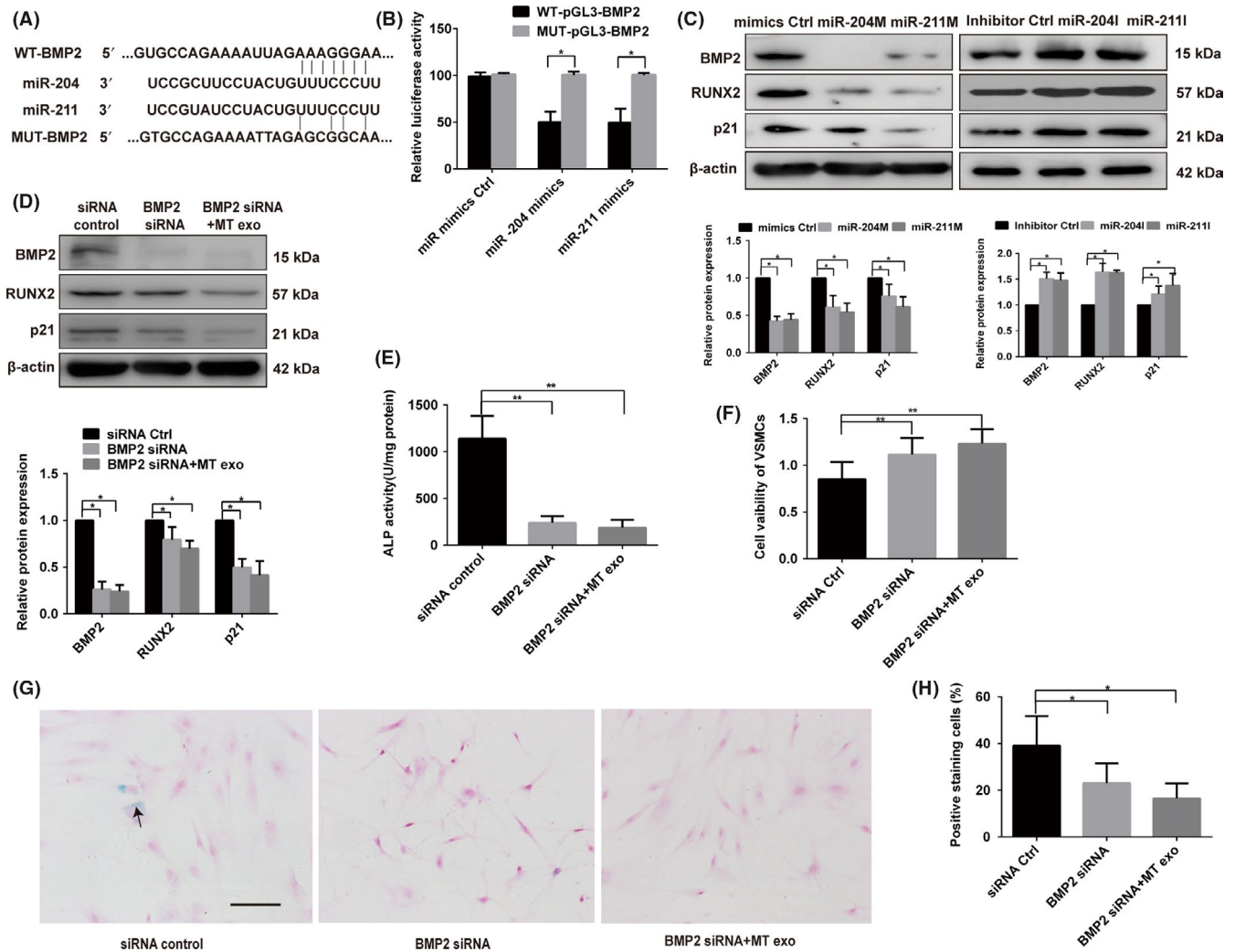


FIGURE 5 BMP2 is the direct target gene of miR-204 and miR-211. A, Schematic representation of miR-204/211 putative target sites in BMP2 3'-UTR and alignment of miR-204/211 with WT and MUT BMP2 3'-UTR showing pairing. B, Luciferase reporter assays were performed using luciferase constructs carrying a WT or mutant BMP2 3'-UTR cotransfected into VSMCs with miR-204/211 mimics compared with an empty vector control. Firefly luciferase activity was normalised to Renilla luciferase activity. C, miR-204/211 mimics or miR-204/211 inhibitor regulated BMP2, RUNX2 and p21 protein expression as indicated by Western blotting. D, Knock-down of BMP2 by siRNA decreased the protein level of BMP2, RUNX2 and p21 as indicated by Western blotting. BMP2 siRNA attenuated the effect of exosomes from MT-treated VSMCs (MT exo) on RUNX2 and p21 expression detected by Western blotting. E, ALP activity was measured with an ALP measurement kit in the VSMCs with BMP2 siRNA group, BMP2 siRNA plus exosomes from MT-treated VSMC group (MT exo) and the siRNA group. F, CCK8 assay was measured in the VSMCs with BMP2 siRNA group, BMP2 siRNA plus exosomes from MT-treated VSMCs (MT exo) and the siRNA group. G and H, VSMCs treat with BMP2 siRNA group, BMP2 siRNA plus exosomes from MT-treated VSMCs (MT exo) and siRNA group then subjected to SA-β-gal staining. Semi-quantitative analyses of SA-β-gal-positive cells were performed. Representative microscopic views are shown. Scale bar represents 200 μm. Three independent experiments were performed, and representative data are shown. The data represent the mean ± SD. NC, normal control. * $P < .05$, ** $P < .01$

staining of VSMCs was also significantly decreased following transfection of BMP2 siRNA in VSMCs (Figure 5G). We then added exosomes derived from VSMCs treated with MT to the BMP2 siRNA group. Notably, the effects of exosomes on osteogenesis and senescence of VSMCs were BMP2-dependent, evidenced by the ability of BMP2 knockdown to attenuate the effects of exosomes from MT-treated VSMCs on the osteogenic differentiation and senescence of VSMCs (Figure 5D-H). These results demonstrated that BMP2 is involved in the osteogenic differentiation and senescence of VSMCs,

and exosomes may mediate this protective effect through the BMP2 pathway.

3.7 | Exosomes mediate MT-induced inhibition effects on vascular calcification and ageing in 5/6 NTP mouse model

To elucidate the effect of MT on vascular calcification in vivo, we first performed 5/6 nephrectomy in C57BL/6 mice and

followed with a high-phosphate diet (5/6 NTP) throughout the study to develop uraemia-induced vascular calcification. Given that arterial calcification is the well-known phenotype of arterial ageing³⁸⁻⁴⁰ and that end-stage renal failure goes along with progressive vascular ageing,^{41,42} we also used this mouse model to study the ageing state of arteries. In 5/6 NTP-induced mice, MT was injected via *i.p.* every day for 4 weeks with vehicle-injected mice as the negative control group (Figure 6A). To evaluate the aortic calcification, Von Kossa staining, Alizarin Red S staining, measurement of calcium content and the ALP activity, as well as detection of RUNX2 expression in the thoracic aorta tissue, were performed. Our data showed that 5/6 NTP-induced mice had significantly higher calcium content (Figure 6B) and the ALP activity (Figure 6C), Von Kossa staining and Alizarin Red S staining level (Figure 6D) as well as RUNX2 expression (Figure 6E) compared to the sham group, suggesting the successful establishment of mouse calcification model. Meanwhile, ageing-associated markers such as SA- β -gal staining level (Figure 6F) and p21 expression (Figure 6J) were increased in the thoracic aorta tissue of 5/6 NTP-induced mice than these of sham control mice, indicating accelerating ageing in calcification mice. Moreover, in 5/6 NTP-induced mice, calcium content (Figure 6B), ALP activity (Figure 6C), Von Kossa staining and Alizarin Red S staining level (Figure 6D), as well as RUNX2 expression (Figure 6E) in thoracic aorta compared with those of the vehicle control group, suggest that MT alleviates 5/6 NTP-induced vascular calcification *in vivo*. However, the addition of GW4869 partially reversed the inhibition of MT on calcium content (Figure 6B), ALP activity (Figure 6C), Von Kossa staining and Alizarin Red S staining level (Figure 6D), as well as RUNX2 expression (Figure 6E), indicating that exosomes partially mediate the MT-induced inhibition effects on vascular calcification. In consistent, ageing-associated markers, such as SA- β -gal staining level (Figure 6F) and p21 expression (Figure 6J), were reduced in the thoracic aorta tissue in 5/6 NTP-induced mice treated with MT compared to those in vehicle-treated mice and these changes were partially abolished by GW4869. Taken together, these data suggest that MT attenuates vascular calcification and ageing in 5/6 NTP-induced mice, which is partially mediated by exosomes.

3.8 | VSMCs^{Mel}-exos containing miR-204/miR-211 prevent vascular calcification and ageing in 5/6 NTP mouse model

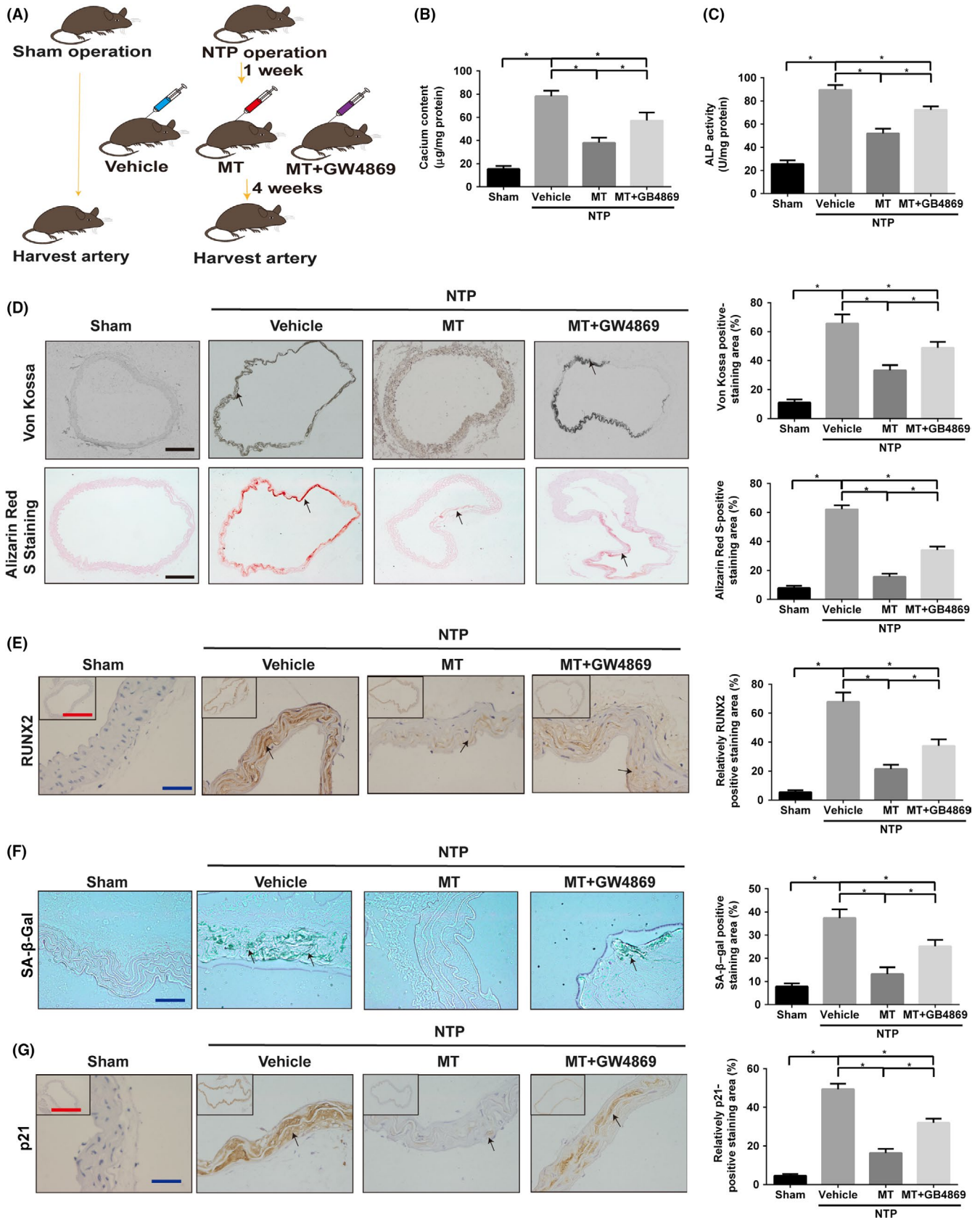
Exosomes have been now been implicated as novel cell-to-cell communication method to transport bioinformation molecules such as miRNAs and proteins. Given that MT-treated VSMC-derived exosomes (VSMCs^{MT}-exos) and exosomal miR-204/miR-211 show inhibition effects on VSMC calcification and senescence *in vitro*, we hypothesised that VSMCs^{MT}-exos could also be incorporated by mouse aortic

VSMCs and reduced vascular calcification and ageing in 5/6 NTP mouse model.

DiR-labelled VSMC exosomes were injected into mouse tail veins to track its distribution in mice. The fluorescence was mainly distributed in the liver (Figure 7A), with little but observable fluorescence in isolated thoracic aorta tissues (Figure 7B). Moreover, injections of both VSMCs^{MT}-exos and VSMCs^{Veh}-exos significantly increased the exosome marker TSG101 expression in VSMCs of thoracic aorta (Figure 7C), demonstrating that exogenous VSMC-derived exosomes could be taken up by mouse thoracic aorta. Meanwhile, VSMCs^{MT}-exos increased the expression of miR-204 and miR-211 in thoracic aorta when compared with VSMCs^{Veh}-exos (Figure 7D). Vascular calcification and ageing markers were also examined after the treatment of VSMC-derived exosomes and flow diagram of treatment was presented in Figure 7E. As shown in Figure 7F,G, calcium content and the ALP activity of thoracic aorta of 5/6 NTP-induced mice were significantly down-regulated by VSMCs^{MT}-exos treatment when compared to VSMCs^{Veh}-exos treatment. Accordingly, Von Kossa staining and Alizarin Red S staining levels, as well as RUNX2 expression in thoracic aorta, were dramatically reduced after the treatment of VSMCs^{MT}-exos (Figure 7H,I). Moreover, VSMCs^{MT}-exos treatment markedly decreased SA- β -gal staining level and p21 expression in thoracic aortic sections, when compared with those of VSMCs^{Veh}-exos-treated mice (Figure 7J,K). These results strongly demonstrate that VSMCs^{MT}-exos can be internalised into mouse VSMCs and thus alleviate vascular calcification and ageing. To further determine whether miR-204 and miR-211 contribute to these effects, we knocked down the expression of miR-204 and miR-211 in VSMCs by miR-204 and miR-211 inhibitor, respectively, followed by MT treatment and exosome isolation. Intriguingly, knockdown of the expression of miR-204 or miR-211 in VSMCs^{MT}-exos partially reversed the inhibition effects of VSMCs^{MT}-exos on calcium content, ALP activity and RUNX2 expression in thoracic aorta, as well as Von Kossa staining and Alizarin Red S staining level of thoracic aortic sections (Figure 7F-I). Meanwhile, knock-down of miR-204 and miR-211 also largely abolished VSMCs^{MT}-exos-induced inhibition effects on SA- β -gal staining level and p21 expression in thoracic aortic sections (Figure 7J,K). Collectively, these data demonstrate that the inhibition effects of VSMCs^{MT}-exos on vascular calcification and ageing are mediated by VSMCs^{MT}-exos containing miR-204/miR-211.

4 | DISCUSSION

In the present study, we found that exosomes mediated MT attenuation of vascular calcification and ageing in a



paracrine manner. Moreover, exosomal miR-204/miR-211 played an important role in this effect (Figure 8). MT can antagonise VSMC osteogenic differentiation and

senescence through an exosome paracrine mechanism. In addition, we clarified that exosomes could carry miR-204/miR-211 to attenuate VSMC osteogenic differentiation

and senescence by targeting BMP2. Of note, we demonstrated that MT and VSMCs^{MT}-exos alleviate vascular calcification and ageing in a 5/6 NTP mouse model, which is partially dependent on exosomal miR-204/miR-211. This analysis revealed a novel finding that has shed light on the molecular mechanism underlying vascular calcification and ageing.

In recent years, MT has been demonstrated to influence the cardiovascular system.⁴³ A significant reduction in endogenous MT secretion may associate with ageing. MT can antagonise premature senescence of cardiac progenitor cells through the H19/miR-675/USP10 signalling pathway.¹⁸ Moreover, a variety of tissues express the MT membrane receptor. MT has been reported to play its biological effects in an MT receptor-dependent or MT receptor-independent manner.^{44,45} The medial artery layer is mainly composed of VSMCs interspersed within elastic fibres. Calcification and ageing of the middle vascular membrane are closely related to phenotypic conversion, differentiation and apoptosis of VSMCs. In this study, we demonstrated that MT could antagonise VSMC osteogenic differentiation and senescence in an MT membrane receptor-dependent manner. Of note, our present investigation confirms supplementation of MT alleviates vascular calcification and ageing in a 5/6 NTP-induced mouse model. These findings provide novel evidence that MT may function as anti-calcification and anti-ageing protein in blood vessels.

By exchange of material such as RNAs, miRNAs, proteins and delivering information, exosomes have been viewed as important mediators of cell-cell communication.⁴⁶ Recipient cells can recycle exosomes back to the extracellular milieu after being taken up by endocytosis.^{47,48} A recent study indicated the paracrine effects of endothelial exosomes.²⁴ In this study, the exosomes were identified using morphology, size and exosomal markers. Our results showed that ALIX and Synt1 were strongly enriched in exosomes from VSMCs, which indicated that the biogenesis of exosomes is dependent on endosomal sorting complex required for transport (ESCRT). Moreover, these exosomes were taken up by VSMCs, evidenced by PKH26 labelled exosomes. We verified that exosomes isolated from MT-treated VSMCs or CVSMCs might suppress

osteogenic differentiation and senescence of these two types of VSMCs, respectively. In addition, the MT-VSMCs-CM group could attenuate the osteogenic differentiation and senescence of VSMCs compared with the MT-VSMCs-GW4869-CM and MT-VSMCs-ex-free-CM groups. The Transwell assay showed that RUNX2 expression and ALP activity in the upper chamber VSMCs were increased in the MT plus GW4869-treated groups compared with the MT plus vehicle group. This data indicated that MT could suppress the osteogenic differentiation and senescence of VSMCs through an exosome paracrine mechanism. Previous work has shown that ex vivo adipose tissue-derived exosomes could be internalised into VSMCs in vivo as demonstrated by increased exosome biomarker CD63 in artery VSMCs.⁴⁹ Interestingly, our present showed that VSMCs^{MT}-exos were demonstrated to be internalised into mouse VSMCs in vivo. Particularly, by using a 5/6 NTP-induced mouse calcification model, we also found that injections of exosomes derived from MT-treated VSMCs into mice strongly reduced calcium content, ALP activity, Von Kossa staining level and RUNX2 expression in thoracic aorta compared with those of exosomes derived from vehicle-treated VSMCs. Meanwhile, VSMCs^{MT}-exos markedly decreased p21 expression and SA- β -gal staining in thoracic aorta. However, inhibition of exosomes by GW4869 partially reversed MT-induced downregulation of ageing-associated phenotypes and calcification in the thoracic aorta of the 5/6 NTP mouse model. Therefore, exosomes mediate MT-induced anti-calcification and anti-ageing functions in the aorta and could be used as an efficient cargo to transport biological information.

More recently, miR-204 and miR-211, which are encoded as a gene cluster, were found to target RUNX2 and important in regulating the VSMC phenotype.⁴ It is known that these two miRs, negative regulators of osteoblast differentiation and subsequent mineralisation, functionally inhibited the differentiation of osteoprogenitors by attenuating the essential transcription factor RUNX2.⁵⁰ We found that MT can increase the expression level of miR-204 and miR-211 in VSMCs and their exosomes. To further confirm that exosomal miR-204 and miR-211 antagonise VSMC osteogenic differentiation and senescence, we isolated the

FIGURE 6 MT alleviates vascular calcification and ageing in the 5/6 NTP-induced mouse model. A, Schematic flow diagram representing the in vivo treatment of MT with or without GW4869 in the 5/6 NTP mouse model. Sham operation mice with high-phosphate diet were used as control (n = 5 per group). B, Calcium content of the thoracic aorta of mice was measured by o-cresolphthalein complexone method. C, The ALP activity of thoracic aortic tissues was measured by the specific kit and normalised to total proteins contents. D, Representative microscopic pictures of Von Kossa-stained and Alizarin Red S-stained sections from the thoracic aorta (left panel) and quantitation of positive staining area (right panel) are shown. Scale bar 200 μ m (Black). E, The expression of RUNX2 in thoracic aorta was examined by immunohistochemistry (IHC) (left panel), and quantitation of positive staining area (right panel) is shown. Scale bar 50 μ m (Blue) and 500 μ m (Red). F, Representative vascular SA- β -gal staining pictures are presented (left panel), and quantitation of positive staining area (right panel) is shown. Scale bar 50 μ m (Blue). Green staining area indicates ageing tissues. G, The expression of p21 in thoracic aorta was determined by immunohistochemistry (left panel), and quantitation of positive staining area (right panel) is shown. Scale bar 50 μ m (Blue) and 500 μ m (Red). Results are represented by mean \pm SEM with five replicates for each group. Significance was analysed by two-way ANOVA with Tukey's HSD post hoc analysis. **P* < .05

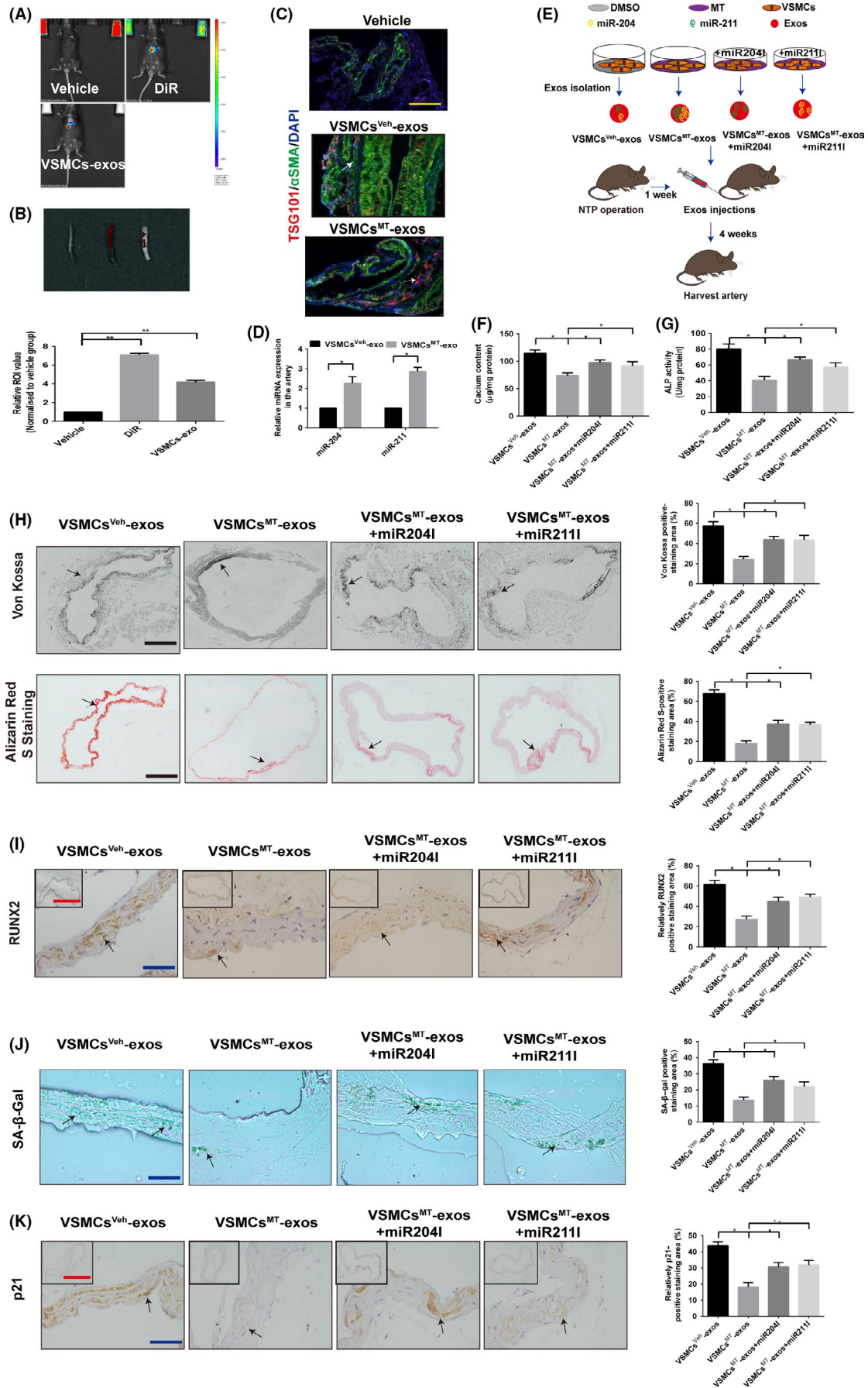


FIGURE 7 Exosomal miR-204/miR-211 contributes to the inhibition effects of VSMCs^{MT}-exos on vascular calcification and ageing in a 5/6 NTP mouse model. A, The 5/6 NTP-induced mice were subjected to vehicle (sterile PBS), DiR or DiR-labelled VSMC-derived exosomes (VSMCs-exos) intravenously (100 µg/mice, n = 5 per group). Representative *in vivo* images of mice (A) and *ex vivo* images of thoracic aorta (B, upper panel), as well as quantification of fluorescence intensities in thoracic aorta (B, lower panel), are shown after treatment for 24 h. (C and D) Exosomes from MT-treated VSMCs (VSMCs^{MT}-exos, 100 µg/mice) or vehicle-treated VSMCs (VSMCs^{Veh}-exos, 100 µg/mice) were injected intravenously every 3 d for 4 wk in 5/6 NTP mice (n = 5 per group). C, Representative confocal fluorescence images of exosome marker TSG101 (red fluorescence) and smooth muscle marker αSMA (green fluorescence) in thoracic aorta sections are shown. Scale bar represents 50 µm (yellow). D, Relative expression of miR-204 and miR-211 in the artery was detected by qRT-PCR. E, Schematic flow diagram of injections of exosomes with or without miR-204 and miR-211 in 5/6 NTP-induced mice (n = 5 per group). F, Calcium content of thoracic aorta of mice was measured by o-cresolphthalein complexone method. G, The ALP activity of thoracic aortic tissues normalised to total proteins contents. H, Von Kossa-stained and Alizarin Red S-stained sections from thoracic aorta (left panel) and quantitation of positive staining area (right panel) are shown. Scale bar 200 µm (Black). I, Immunohistochemistry analysis of RUNX2 in thoracic aorta (left panel) and quantitation of positive staining area (right panel) are shown. Scale bar 50 µm (Blue) and 500 µm (Red). J, SA-β-gal-stained (Green) micrographs are presented (left panel), and quantitation of positive staining area (right panel) is shown. Scale bar 50 µm (Blue). Green staining area indicates ageing tissues. K, Immunohistochemistry analysis of the expression of p21 in thoracic aorta (left panel) and quantitation of positive staining area (right panel) are shown. Scale bar 50 µm (Blue) and 500 µm (Red). Results are represented by mean ± SEM with five replicates for each group. Significance was analysed by two-way ANOVA with Tukey's HSD post hoc analysis. **P* < .05

exosomes from overexpressed miR-204 or miR-211 VSMCs and found these exosomes from overexpression miR-204 or miR-211 VSMCs suppressed the osteogenic differentiation and senescence of VSMCs. At the same time, exosomes from overexpression miR-204 or miR-211 VSMCs also increased the proliferation of VSMCs as shown by the CCK8 assay. We also examined the role of exosomal miR-204 and miR-211 in vascular calcification and ageing. Interestingly, knock-down of miR-204 and miR-211 in VSMCs largely abolished VSMCs^{MT}-exos-induced inhibition effects on calcification and ageing phenotypes in the artery of 5/6 NTP-induced mouse model. These results were consistent with previous findings that exosomal miRNAs mediate crosstalk inter-cells and inter-organs.^{51,52} These data indicate that MT induced exosomal miR-204 and miR-211 to antagonise vascular calcification and ageing both *in vitro* and *in vivo*.

BMP2 is a local growth factor and is the only growth factor which can induce bone formation alone. Recent findings in VSMCs have suggested that BMP2 promotes vascular calcification by inducing apoptosis.⁵³ Senescent VSMCs tend to be a phenotype predisposing vascular tissue to calcification.⁵⁴ Moreover, this study found that senescent VSMCs induced expression of BMP2, indicating that BMP2 is involved in the senescence of VSMCs. In the present study, we used several bioinformatic target prediction algorithms and a luciferase reporter assay to confirm that BMP2 is a target of miR-204 and miR-211. Western blot analysis revealed that overexpression of miR-204 and miR-211 reduced the expression of BMP2. The expression of BMP2 decreased significantly in miR-204 and miR-211 inhibitor-transfected cells compared with control.

It has been reported that the senescent VSMCs gain an osteoblast-like phenotype and decreased sensitivity to BMP2.⁵³ However, the molecular mechanism of BMP2 in vascular calcification and ageing has remained unclear. Therefore, we

investigated the effect of BMP2 knock-down by siRNA in VSMCs. As expected, RUNX2 expression and ALP activity were significantly downregulated following knock-down BMP2 in VSMCs; senescence of VSMCs was decreased at the same time. Moreover, BMP2 knock-down attenuated the effect of exosomes from MT-treated VSMCs on VSMC osteogenic differentiation and senescence, which showed BMP2 mediated the exosome effect on osteogenic differentiation and senescence of VSMCs.

Our present study revealed that the MT-treated VSMCs secreting exosomal miR-204/miR-211 played a paracrine effect in vascular calcification and ageing both *in vivo* and *in vitro*. Our results indicate that MT can potentially be used in the therapy of vascular calcification and ageing by targeting exosomal miR-204/miR-211. Furthermore, understanding of the intricate regulatory network of exosomal miR-204/miR-211 and BMP2 may allow for the development of effective therapies for the prevention of vascular calcification and ageing.

CONFLICT OF INTEREST

The authors declare no conflict of interest.

ORCID

Ling-Qing Yuan  <https://orcid.org/0000-0001-8602-7113>

REFERENCES

- Shanahan CM, Crouthamel MH, Kapustin A, Giachelli CM. Arterial calcification in chronic kidney disease: key roles for calcium and phosphate. *Circ Res*. 2011;109(6):697-711.
- Huang J, Huang H, Wu M, et al. Connective tissue growth factor induces osteogenic differentiation of vascular smooth muscle cells through ERK signaling. *Int J Mol Med*. 2013;32(2):423-429.
- Lanzer P, Boehm M, Sorribas V, et al. Medial vascular calcification revisited: review and perspectives. *Eur Heart J*. 2014;35(23):1515.
- Panizo S, Naves-Diaz M, Carrillo-Lopez N, et al. MicroRNAs 29b, 133b, and 211 regulate vascular smooth muscle

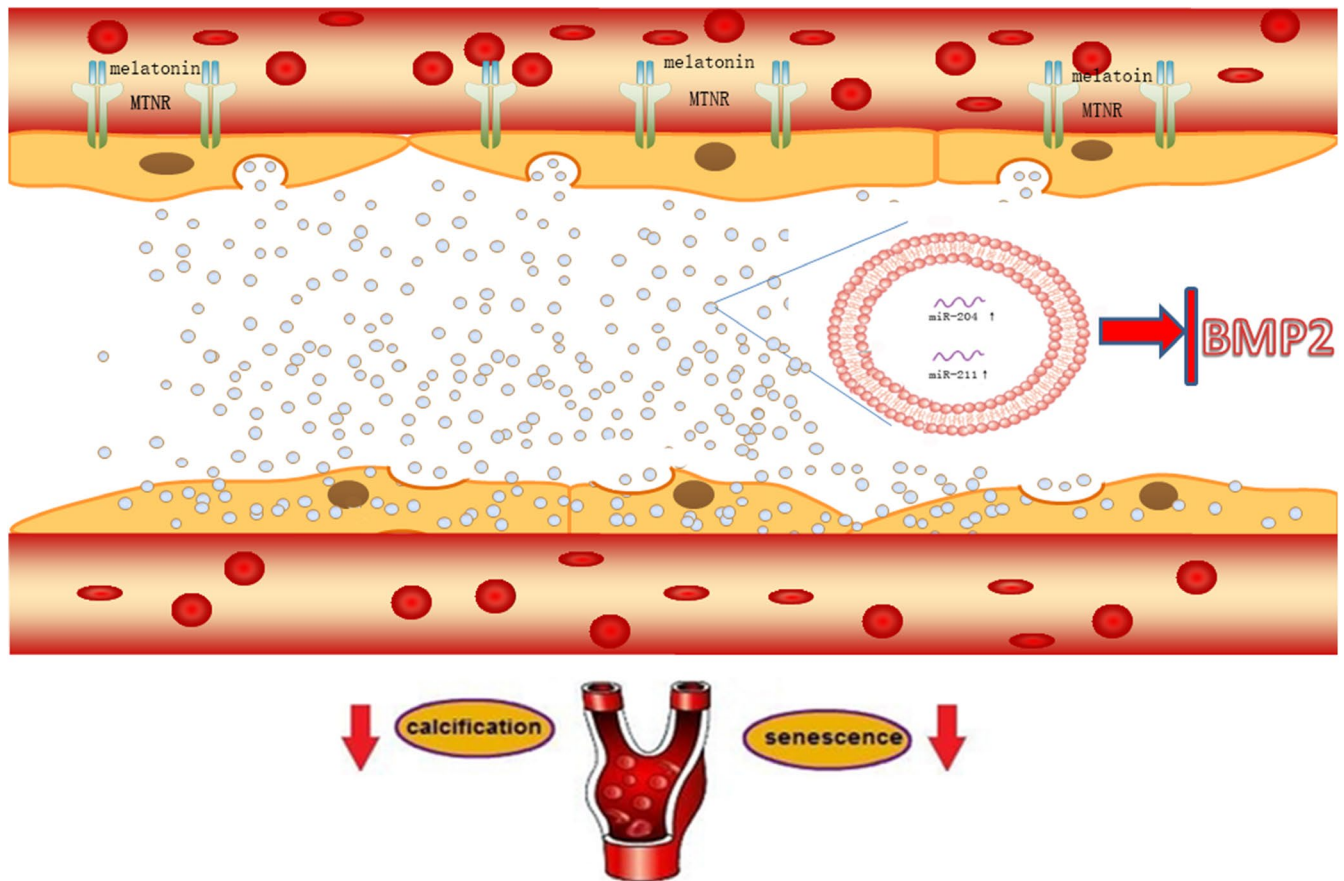


FIGURE 8 The mechanism diagram about exosomes from MT-treated VSMCs could attenuate vascular calcification and ageing in a paracrine manner through an exosomal miR-204/miR-211. MT can antagonise VSMC osteogenic differentiation and senescence through exosome paracrine mechanism. In addition, MT-treated VSMCs can secrete exosomal miR-204/miR-211 to antagonise VSMC osteogenic differentiation and senescence as well as vascular calcification and ageing. BMP2 was revealed to be a potential target of miR-204 and miR-211 and increased VSMC osteogenic differentiation and senescence

- calcification mediated by high phosphorus. *J Am Soc Nephrol.* 2015;27(3):824-834.
- Rodriguez A, Fruhbeck G, Gomez-Ambrosi J, et al. The inhibitory effect of leptin on angiotensin II-induced vasoconstriction is blunted in spontaneously hypertensive rats. *J Hypertens.* 2006;24(8):1589-1597.
 - Zhan JK, Tan P, Wang YJ, et al. Exenatide can inhibit calcification of human VSMCs through the NF-kappaB/RANKL signaling pathway. *Cardiovasc Diabetol.* 2014;13:153.
 - Doi H, Iso T, Yamazaki M, et al. HERP1 inhibits myocardium-induced vascular smooth muscle cell differentiation by interfering with SRF binding to CARG box. *Arterioscler Thromb Vasc Biol.* 2005;25(11):2328-2334.
 - Kapustin AN, Schoppet M, Schurgers LJ, et al. Prothrombin loading of vascular smooth muscle cell-derived exosomes regulates coagulation and calcification. *Arterioscler Thromb Vasc Biol.* 2017;37(3):e22-e32.
 - Zhao W, Zheng XL, Zhao SP. Exosome and its roles in cardiovascular diseases. *Heart Fail Rev.* 2015;20(3):337-348.
 - Wu F, Li F, Lin X, et al. Exosomes increased angiogenesis in papillary thyroid cancer microenvironment. *Endocr Relat Cancer.* 2019;26(5):525-538.
 - Li S, Zhan JK, Wang YJ, et al. Exosomes from hyperglycemia-stimulated vascular endothelial cells contain versican that regulate calcification/senescence in vascular smooth muscle cells. *Cell Biosci.* 2019;9:1.
 - Lehmann BD, Paine MS, Brooks AM, et al. Senescence-associated exosome release from human prostate cancer cells. *Can Res.* 2008;68(19):7864-7871.
 - Manchester LC, Coto-Montes A, Boga JA, et al. Melatonin: an ancient molecule that makes oxygen metabolically tolerable. *J Pineal Res.* 2015;59(4):403-419.
 - Pandi-Perumal SR, BaHammam AS, Ojike NI, et al. Melatonin and human cardiovascular disease. *J Cardiovasc Pharmacol Ther.* 2017;22(2):122-132.
 - Dwaich KH, Al-Amran FG, Al-Sheibani BI, Al-Aubaidy HA. Melatonin effects on myocardial ischemia-reperfusion injury: impact on the outcome in patients undergoing coronary artery bypass grafting surgery. *Int J Cardiol.* 2016;221:977-986.
 - Dominguez-Rodriguez A, Abreu-Gonzalez P, Piccolo R, Galasso G, Reiter RJ. Melatonin is associated with reverse remodeling after cardiac resynchronization therapy in patients with heart failure and ventricular dyssynchrony. *Int J Cardiol.* 2016;221:359-363.
 - Dominguez-Rodriguez A, Abreu-Gonzalez P, Sanchez-Sanchez JJ, Kaski JC, Reiter RJ. Melatonin and circadian biology in human cardiovascular disease. *J Pineal Res.* 2010;49(1):14-22.

18. Cai B, Ma W, Bi C, et al. Long noncoding RNA H19 mediates melatonin inhibition of premature senescence of c-kit(+) cardiac progenitor cells by promoting miR-675. *J Pineal Res.* 2016;61(1):82-95.
19. Tkach M, Thery C. Communication by extracellular vesicles: where we are and where we need to go. *Cell.* 2016;164(6):1226-1232.
20. Valadi H, Ekstrom K, Bossios A, Sjostrand M, Lee JJ, Lotvall JO. Exosome-mediated transfer of mRNAs and microRNAs is a novel mechanism of genetic exchange between cells. *Nat Cell Biol.* 2007;9(6):654-659.
21. Yin W, Ouyang S, Luo Z, et al. Immature exosomes derived from MicroRNA-146a overexpressing dendritic cells act as antigen-specific therapy for myasthenia gravis. *Inflammation.* 2017;40(4):1460-1473.
22. Wang J, Deng Z, Wang Z, et al. MicroRNA-155 in exosomes secreted from helicobacter pylori infection macrophages immunomodulates inflammatory response. *Am J Transl Res.* 2016;8(9):3700-3709.
23. Li FX, Liu JJ, Xu F, et al. Role of tumor-derived exosomes in bone metastasis. *Oncol Lett.* 2019;18(4):3935-3945.
24. van Balkom BW, de Jong OG, Smits M, et al. Endothelial cells require miR-214 to secrete exosomes that suppress senescence and induce angiogenesis in human and mouse endothelial cells. *Blood.* 2013;121(19):3997-4006, s3991-s3915.
25. Peng-Fei S, Ying L, Rong-Rong C, Yi J, Ling-Qing Y, Er-Yuan L. Apelin attenuates the osteoblastic differentiation of vascular smooth muscle cells. *PLoS ONE.* 2011;6(3):e17938.
26. Liao XB, Zhang ZY, Yuan K, et al. MiR-133a modulates osteogenic differentiation of vascular smooth muscle cells. *Endocrinology.* 2013;154(9):3344-3352.
27. Zhou W, Fong MY, Min Y, et al. Cancer-secreted miR-105 destroys vascular endothelial barriers to promote metastasis. *Cancer Cell.* 2014;25(4):501-515.
28. Lin X, Xu F, Cui R-R, et al. Arterial calcification is regulated via an miR-204/DNMT3a regulatory circuit both in vitro and in female mice. *Endocrinology.* 2018;159(8):2905-2916.
29. Ali T, Badshah H, Kim TH, Kim MO. Melatonin attenuates D-galactose-induced memory impairment, neuroinflammation and neurodegeneration via RAGE/NF-K B/JNK signaling pathway in aging mouse model. *J Pineal Res.* 2015;58(1):71-85.
30. Dinkins MB, Dasgupta S, Wang G, Zhu G, Bieberich E. Exosome reduction in vivo is associated with lower amyloid plaque load in the 5XFAD mouse model of Alzheimer's disease. *Neurobiol Aging.* 2014;35(8):1792-1800.
31. Lin X, Li F, Xu F, et al. Aberration methylation of miR-34b was involved in regulating vascular calcification by targeting Notch1. *Aging.* 2019;11(10):3182-3197.
32. Xu F, Li FX, Lin X, et al. Adipose tissue-derived omentin-1 attenuates arterial calcification via AMPK/Akt signaling pathway. *Aging.* 2019;11(20):8760-8776.
33. Luo XH, Zhao LL, Yuan LQ, Wang M, Xie H, Liao EY. Development of arterial calcification in adiponectin-deficient mice: adiponectin regulates arterial calcification. *J Bone Miner Res.* 2009;24(8):1461-1468.
34. Orita Y, Yamamoto H, Kohno N, et al. Role of osteoprotegerin in arterial calcification: development of new animal model. *Arterioscler Thromb Vasc Biol.* 2007;27(9):2058-2064.
35. Cui RR, Li SJ, Liu LJ, et al. MicroRNA-204 regulates vascular smooth muscle cell calcification in vitro and in vivo. *Cardiovasc Res.* 2012;96(2):320-329.
36. Hu Y, Baker AH, Zou Y, Newby AC, Xu Q. Local gene transfer of tissue inhibitor of metalloproteinase-2 influences vein graft remodeling in a mouse model. *Arterioscler Thromb Vasc Biol.* 2001;21(8):1275-1280.
37. Chen G, Huang AC, Zhang W, et al. Exosomal PD-L1 contributes to immunosuppression and is associated with anti-PD-1 response. *Nature.* 2018;560(7718):382-386.
38. Tesaro M, Mauriello A, Rovella V, et al. Arterial ageing: from endothelial dysfunction to vascular calcification. *J Intern Med.* 2017;281(5):471-482.
39. Kockelkoren R, De Vis JB, de Jong PA, et al. Intracranial carotid artery calcification from infancy to old age. *J Am Coll Cardiol.* 2018;72(5):582-584.
40. Wang J, Uryga AK, Reinhold J, et al. Vascular smooth muscle cell senescence promotes atherosclerosis and features of plaque vulnerability. *Circulation.* 2015;132(20):1909-1919.
41. London GM, Safar ME, Pannier B. Aortic aging in ESRD: structural, hemodynamic, and mortality implications. *J Am Soc Nephrol: JASN.* 2016;27(6):1837-1846.
42. Kooman JP, Kotanko P, Schols AM, Shiels PG, Stenvinkel P. Chronic kidney disease and premature ageing. *Nat Rev Nephrol.* 2014;10(12):732-742.
43. Yang Y, Sun Y, Yi W, et al. A review of melatonin as a suitable antioxidant against myocardial ischemia-reperfusion injury and clinical heart diseases. *J Pineal Res.* 2014;57(4):357-366.
44. Sei-Jung L, Young Hyun J, Yub OS, Seung Pil Y, Ho JH. Melatonin enhances the human mesenchymal stem cells motility via melatonin receptor 2 coupling with Gαq in skin wound healing. *J Pineal Res.* 2015;57(4):393-407.
45. Tocharus C, Puriboriboon Y, Junmanee T, Tocharus J, Ekthuwapranee K, Govitrapong P. Melatonin enhances adult rat hippocampal progenitor cell proliferation via ERK signaling pathway through melatonin receptor. *Neuroscience.* 2014;275(13):314-321.
46. Camussi G, Deregibus MC, Bruno S, Cantaluppi V, Biancone L. Exosomes/microvesicles as a mechanism of cell-to-cell communication. *Kidney Int.* 2010;78(9):838-848.
47. Milane L, Singh A, Mattheolabakis G, Suresh M, Amiji MM. Exosome mediated communication within the tumor microenvironment. *J Controlled Release Off J Controlled Release Soc.* 2015;219:278-294.
48. Chen CY, Rao SS, Ren L, et al. Exosomal DMBT1 from human urine-derived stem cells facilitates diabetic wound repair by promoting angiogenesis. *Theranostics.* 2018;8(6):1607-1623.
49. Li X, Ballantyne LL, Yu Y, Funk CD. Perivascular adipose tissue-derived extracellular vesicle miR-221-3p mediates vascular remodeling. *FASEB J: Off Publ Federation Am Soc Exp Biol.* 2019;33(11):12704-12722.
50. Wang Y, Chen S, Deng C, et al. MicroRNA-204 targets Runx2 to attenuate BMP-2-induced osteoblast differentiation of human aortic valve interstitial cells. *J Cardiovasc Pharmacol.* 2015;66(1):63-71.
51. Deng L, Blanco FJ, Stevens H, et al. MicroRNA-143 activation regulates smooth muscle and endothelial cell crosstalk in pulmonary arterial hypertension. *Circ Res.* 2015;117(10):870-883.
52. Thomou T, Mori MA, Dreyfuss JM, et al. Adipose-derived circulating miRNAs regulate gene expression in other tissues. *Nature.* 2017;542(7642):450-455.
53. Nakano-Kurimoto R, Ikeda K, Uraoka M, et al. Replicative senescence of vascular smooth muscle cells enhances the calcification

through initiating the osteoblastic transition. *Am J Physiol Heart Circ Physiol.* 2009;297(5):H1673-H1684.

54. Burton DG, Giles PJ, Sheerin AN, et al. Microarray analysis of senescent vascular smooth muscle cells: a link to atherosclerosis and vascular calcification. *Exp Gerontol.* 2009;44(10):659-665.

SUPPORTING INFORMATION

Additional supporting information may be found online in the Supporting Information section.

How to cite this article: Xu F, Zhong J-Y, Lin X, et al. Melatonin alleviates vascular calcification and ageing through exosomal miR-204/miR-211 cluster in a paracrine manner. *J Pineal Res.* 2020;68:e12631. <https://doi.org/10.1111/jpi.12631>